ISME

An Analytical Study for Nonlinear Vibration Analysis of Two-directional Functionally Graded Rectangular Plate

S. Hashemi*
M.Sc. Student

A.A. Jafari†
Professor

In this study, an analytical solution is presented for investigating the nonlinear vibration analysis of two-directional functionally graded rectangular plate for the first time. On the basis of first order shear deformation theory (FSDT) and Galerkin procedure, the equations of motion are developed. The nonlinear equation of motion is then solved analytically by modified Lindstedt-Poincare method. The volume fraction distribution is assumed to be symmetrical for characterizing the in-plane material inhomogeneity. Finally, the effects of some system parameters such as non-dimensional vibration amplitude, volume fraction indexes and aspect ratio on the nonlinear to linear frequency ratio are discussed in detail. To validate the analysis, the results of this paper are compared with the published data and good agreements are found.

DOI: 10.30506/jmee.2020.112273.1193

Keywords: Nonlinear vibration; Rectangular plate; bi-directional functionally graded material; First order shear deformation theory; Modified Lindstedt-Poincare method

1 Introduction

Functionally graded materials (FGM) are a type of composite materials whose mechanical and thermal properties change from one surface to another according to a continuous function. The use of FGMs has increased significantly in recent decades. Due to its high thermal resistance and other properties, FGMs have many engineering applications in various industries such as defense industries and aerospace industries. FGMs are commonly used in the construction of equipment such as pressure vessels, turbine blades, heat exchangers, biomaterials like dental implants and etc. Plates are one of the most common FG structures which have many applications in the practical engineering. Therefore, due to their high importance, many studies have been reported on the dynamics of FG plates. Some researchers worked on the vibrations of FG plates based on classical plate theory (CPT). Zhang and Zhou [1] investigated free vibration, deflection and buckling analysis of the FG plates using the CPT based on physical neutral surface. Abrate [2] calculated natural frequencies of FG clamped and simply supported rectangular thin plates based on the CPT. Since rotatory inertia and shear deformation are neglected in the CPT, results given by CPT are admissible only for thin plates.

* M.Sc. Student, Faculty of Mechanical Engineering, K.N. Toosi University of Technology, Tehran, Iran
soheil.hashemi1994@gmail.com

† Corresponding Author, Professor, Department of Mechanical Engineering, K. N. Toosi University of Technology, Tehran, Iran AJafari@Kntu.ac.ir

Receive : 2019/07/31 Accepted : 2020/01/12

As a result, some researchers used first order shear deformation theory (FSDT) to take into account the effects of rotary inertia and shear deformation to analysis of thick plates [3-9]. Hosseini Hashemi et al. [10] presented analytical method for analysis of free vibrations of FG rectangular plate on an elastic foundation using FSDT. By using element free kp-ritz method, Zhao et al. [11] carried out the free vibrations of FG rectangular plate based on FSDT. They considered four types of FGM in their investigation. Yang and Shen [12] analyzed the free and forced vibrations of initially stressed FG plate in thermal environment with different boundary conditions on the basis of the FSDT. Gupta et al. [13] obtained linear frequencies of rectangular plate with different boundary constraint by using FSDT. In addition, some researchers used different theories for their analysis. For example, Arefi et al [14]. used two-variable sinusoidal shear deformation theory for free vibration analysis of a sandwich nano-plate. Based on nonlocal elasticity theory and third order shear deformation theory, Arefi and Rabczuk [15] investigated bending analysis of a piezoelectric doubly curved nano shell. Arefi et al. [16] developed the sinusoidal shear deformation theory and physical neutral surface to analysis of functionally graded piezoelectric plate. Based on higher-order sinusoidal shear deformation beam theory, Arefi and Zenkour [17] studied bending analysis of a sandwich microbeam.

During recent years, many studies have reported on the nonlinear analysis and large amplitude vibration. Some researchers has provided articles on the nonlinear vibrations of FG plates. Yan Qing Wang And Jean W. Zu [18] presented a nonlinear vibrations analysis of FG plates incorporating the porosity. They used Almert's principle to derive the governing partial differential equations of plate and eventually solved it by Harmonic balance method. Ali Amin Yazdi [19] used the homotopy perturbation method to obtain nonlinear to linear frequency ratio of the FG rectangular plate. By using Fourier series, J. Woo et al. [20] investigated the effects of some parameters of the system on the dynamic behavior of FG plate. Malekzadeh and Monajjemzadeh [21] employed the CPT to analyze the nonlinear response of FG plates under moving load. Dinh Duc and Hong Cong [22] used the Runge Kutta method to determine the nonlinear dynamic response of an FG plate resting on elastic foundations that subjected to thermal, mechanical and damping loads. Fung and Chen [23] established nonlinear equations for an imperfect FG plate and then they considered effects of volume fraction index, geometric imperfection and initial stress on nonlinear vibrations. The finite element formulation, based on HSDT, has been developed by Vahid Fakhari et al. [24] to analyze the nonlinear free and forced vibrations of FG plate with surface bonded piezoelectric layers in thermal environment.

Y.X. Hao et al. [25] dealt with the nonlinear dynamic analysis of FG cantilever plate under transversal excitation in thermal environment by using asymptotic perturbation method. They employed Runge-Kutta method and asymptotic perturbation method to obtain the nonlinear dynamic responses of the plate. An asymptotic perturbation method is used by Zhang et al. [26] to investigate the nonlinear responses of FG plate subjected to through the thickness thermal loading combined with external and parametric excitations. Based on HSDT, Duc et al. [27] presented an analysis of the nonlinear vibration of imperfect FG thick plates under blast and thermal load resting on the elastic foundations. For design of some engineering structures such as propulsion systems, one-directional-FGMs can not be so effective and components require advance materials whose properties are changed in two or multi directional simultaneously.

Hence, the two-directional functionally graded materials (2D-FGMs) are introduced and many investigation have been reported on static and dynamic analysis of 2D-FG structures. Some studies have been worked on free and forced vibration analysis of 2D-FG beams [28-33]. Some researchers investigated vibration analysis of 2D-FG shells [34,35]. The number of published papers focused on the vibration analysis of bi-directional FG plates is still very limited. Lieu et al. [36] used NURBS basis functions to model and analyze free vibration and buckling responses of in-plane bi-directional functionally graded (IBFG) plates. By using isogeometric analysis, Lieu et al. [37] studied bending and free vibration analysis of IBFG plate with variable

thickness. By finite annular prism methods,Wu and Yu [38] investigated free vibration analysis of bi-directional FG annular plates. Kumar and Lal [39] calculated natural frequencies of free axisymmetric vibration of two-directional FG annular plates resting on Winkler foundation using differential quadratic method. Shariyat and Alipour [40] employed differential transformation method to obtain a semi analytical solution for free vibration of two-directional FG circular plates resting on two-parameter elastic foundations. Alipour and Shariyat [41] employed a semi analytical solution for free vibration of variable thickness two-directional FG circular plates resting on elastic foundations. Sobhani Aragh et al. [42] studied the three-dimensional free vibration and vibrational displacements characteristics of two-dimensional functionally graded fiber-reinforced (2-D FGFR) curved panels with different boundary conditions. By using Chebyshev collocation technique and differential quadrature method, Kumar [43] analyzed free vibration of two-directional FG annular plates. On the basis of classical plates theory and first order shear deformation theory, Lal and Ahlawat [44,45] studied buckling and vibrations of two-directional FG circular plates subjected to hydrostatic in-plane force. Shariyat and Alipour [46] developed a power series solution for free vibration and damping analysis of viscoelastic two-directional FG plates with variable thickness on elastic foundations. Tahouneh and Naei [47] analyzed three dimensional dynamic of bi-directional FG rectangular plates resting on two-parameter elastic foundations based on the three dimensional elasticity theory. Tahouneh and Yas [48] presented semi analytical solution for three dimensional vibration analysis of thick multidirectional FG annular sector plates under different boundary supports. Yas and Moloudi [49] studied Three-dimensional free vibration analysis of multi-directional FG piezoelectric annular plates on elastic foundations via state space based differential quadrature method. In many practical engineering problems, FG structures can work in more severe circumstances such as aerospace shuttles and crafts, nuclear plants, implants, etc. Thus, material property variations in two or three directions are demanded in lieu of only one direction as in the conventional FGMs. To meet those real requirements, an exhaustive understanding of their responses under various conditions is necessary. In addition, from the above mentioned literature, most of the studies on vibration of two-directional FG plate are limited to linear case and there is no reported work on nonlinear vibration of two-directional FG rectangular plate. This article is therefore conducted as the first attempt for scientific contributions. In this research, the nonlinear vibrations of two-directional FG rectangular plate are investigated for the first time. For this purpose, firstly, the partial differential equations of motion are developed based on first order shear deformation theory and von Karman nonlinearity strain displacement relations. Afterward, by applying Galerkin method, the nonlinear partial differential equations are transformed into nonlinear ordinary differential equations. Finally, modified Lindstedt-Poincare method is used for solving analytically the nonlinear governing equation of transverse motion. The volume fraction distribution is assumed to be symmetrical for characterizing the in-plane material inhomogeneity. The effects of some key system parameters such as vibration amplitude, volume fraction indexes and aspect ratio on the nonlinear to linear frequency ratio are discussed in detail. The results are in good agreement with those obtained in previously published papers.

2 Geometry and properties of plate

Figure (1) depicts an 2D-FG rectangular plate composed of alumina and aluminium of length a, width b and thickness h which is simply supported on all four sides. The origin of the Cartesian coordinate system is located in the mid-plane of the plate. Material properties P of the 2D-FG plate are assumed to vary continuously alter in the $x-y$ plane according to power law distribution. These properties can be expressed as:

$$P(x,y) = P_c V_c(x,y) + P_m V_m(x,y) \tag{1}$$

If the volume fraction of the ceramic part is Vc and the metallic part is Vm, the sum of all the volume fractions must be one and is written as:

$$V_c + V_m = 1 \tag{2}$$

Based on the power law distribution, the volume fraction of a 2D-FGM plate is supposed to change continually alter in the $x-y$ plane in the following form:

$$V_c(x,y) = \left(\frac{x}{a}\right)^n \left(\frac{y}{b}\right)^m, \qquad n,m \geq 0 \tag{3}$$

Where n and m designate the power indexes in the $x-$ and $y-$ axes, respectively.
Material properties have the forms:

$$E(x,y) = E_m + (E_c - E_m)\left(\frac{x}{a}\right)^n \left(\frac{y}{b}\right)^m \tag{4}$$

$$\rho(x,y) = \rho_m + (\rho_c - \rho_m)\left(\frac{x}{a}\right)^n \left(\frac{y}{b}\right)^m \tag{5}$$

Where E and ρ are young's modulus and mass density of the 2D-FG plate, respectively. Material properties used in the 2D-FG plate are listed in Table (1).

3 Equations of motion

The displacement field (u,v,w) of the FG plate according to the FSDT can be expressed as [50]:

$$u(x,y,z,t) = u_0(x,y,t) + z\phi_x(x,y,t) \tag{6}$$

$$v(x,y,z,t) = v_0(x,y,t) + z\phi_y(x,y,t) \tag{7}$$

$$w(x,y,z,t) = w_0(x,y,t) \tag{8}$$

Where u_0, v_0 and w_0 are displacements of any point on the middle surface of the FG plate in the x, y and z directions, respectively. ϕ_x and ϕ_y are rotations about y and x axes, respectively. Assuming large deformations, the von Karman nonlinearity strain-displacement relations are given as follows:

$$\varepsilon_{xx} = \frac{\partial u_0}{\partial x} + \frac{1}{2}\left(\frac{\partial w_0}{\partial x}\right)^2 + z\frac{\partial \phi_x}{\partial x} \tag{9}$$

$$\varepsilon_{yy} = \frac{\partial v_0}{\partial y} + \frac{1}{2}\left(\frac{\partial w_0}{\partial y}\right)^2 + z\frac{\partial \phi_y}{\partial y} \tag{10}$$

$$\gamma_{xy} = \left(\frac{\partial u_0}{\partial y} + \frac{\partial v_0}{\partial x} + \frac{\partial w_0}{\partial x}\frac{\partial w_0}{\partial y}\right) + z\left(\frac{\partial \phi_x}{\partial y}\frac{\partial \phi_y}{\partial x}\right) \tag{11}$$

$$\gamma_{xz} = \frac{\partial w_0}{\partial x} + \phi_x \tag{12}$$

$$\gamma_{yz} = \frac{\partial w_0}{\partial y} + \phi_y \tag{13}$$

The governing equations of the first-order shear deformation theory will be derived using the dynamic version of the principle of virtual displacements:

$$\int_0^T (\delta U + \delta V - \delta K)\, dt = 0 \tag{14}$$

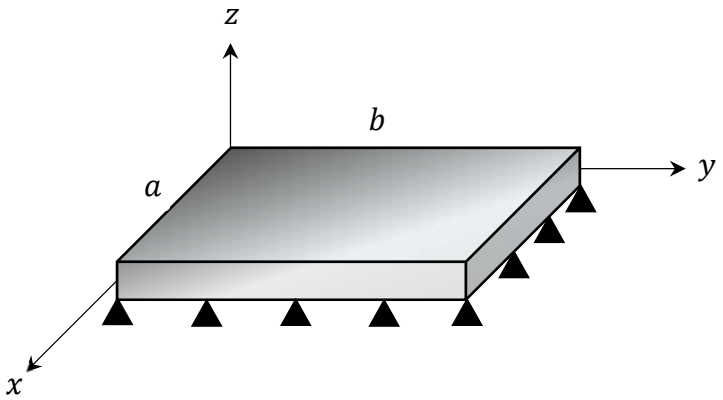

Figure 1 Geometry of a 2D- FG rectangular plate

Table 1 Material properties for 2D-FG plate [50]

Properties	Ceramic (Al_2O_3)	Steel (Al)
Young's module	380 Gpa	70 Gpa
Density	3800 $\frac{Kg}{m^3}$	2702 $\frac{Kg}{m^3}$

Where the virtual strain energy δU, virtual work done by applied forces δV, and the virtual kinetic energy δK are given by:

$$\delta U = \int_{\Omega_0} \left\{ \int_{-\frac{h}{2}}^{+\frac{h}{2}} \left[\sigma_{xx} \left(\delta\varepsilon_{xx}^{(0)} + z\delta\varepsilon_{xx}^{(1)} \right) + \sigma_{yy} \left(\delta\varepsilon_{yy}^{(0)} + z\delta\varepsilon_{yy}^{(1)} \right) + \sigma_{xy} \left(\delta\gamma_{xy}^{(0)} + z\delta\gamma_{xy}^{(1)} \right) + \sigma_{xz}\delta\gamma_{xz}^{(0)} + \sigma_{yz}\delta\gamma_{yz}^{(0)} \right] dz \right\} dxdy \tag{15}$$

$$\delta V = -\int_{\Omega_0} [q\delta w_0] dxdy \tag{16}$$

$$\delta K = \int_{\Omega_0} \left\{ \int_{-\frac{h}{2}}^{+\frac{h}{2}} \rho(x,y) \left[\left(\dot{u}_0 + z\dot{\phi}_x\right)\left(\delta\dot{u}_0 + z\delta\dot{\phi}_x\right) + \left(\dot{v}_0 + z\dot{\phi}_y\right)\left(\delta\dot{v}_0 + z\delta\dot{\phi}_y\right) + \dot{w}_0\delta\dot{w}_0 \right] dzdxdy \right\} \tag{17}$$

Substituting for $\delta U, \delta V,$ and δK from Eq. (15)-(17) into the virtual work statement in Eq. (14) and integrating through the thickness of the 2D-FG plate gives:

$$\int_0^T \left\{ \int_{\Omega_0} \left[N_{xx}\delta\varepsilon_{xx}^{(0)} + M_{xx}\delta\varepsilon_{xx}^{(1)} + N_{yy}\delta\varepsilon_{yy}^{(0)} + M_{yy}\delta\varepsilon_{yy}^{(1)} + N_{xy}\delta\gamma_{xy}^{(0)} + M_{xy}\delta\gamma_{xy}^{(1)} + Q_x\delta\gamma_{xz}^{(0)} + Q_y\delta\gamma_{yz}^{(0)} - q\delta w_0 - I_0(\dot{u}_0\delta\dot{u}_0 + \dot{v}_0\delta\dot{v}_0 + \dot{w}_0\delta\dot{w}_0) - I_1\left(\dot{\phi}_x\delta\dot{u}_0 + \dot{\phi}_y\delta\dot{v}_0 + \delta\dot{\phi}_x\dot{u}_0 + \delta\dot{\phi}_y\delta\dot{v}_0\right) - I_2\left(\dot{\phi}_x\delta\dot{\phi}_x + \dot{\phi}_y\delta\dot{\phi}_y\right) \right] \right\} dxdy \tag{18}$$

Where N, M and Q are called the in-plane force resultants, moments resultants and transverse force resultants, I_0, I_1 and I_2 are inertia related terms and q is the external load which is not considered in free vibrations. The force, moment, transverse force resultant and mass moments of inertia resultants of the 2D-FG plate can be written in terms of stress components across the thickness of the plate:

$$\begin{Bmatrix} N_{xx} \\ N_{yy} \\ N_{xy} \end{Bmatrix} = \int_{-\frac{h}{2}}^{+\frac{h}{2}} \begin{Bmatrix} \sigma_{xx} \\ \sigma_{yy} \\ \tau_{xy} \end{Bmatrix} dz \tag{19}$$

$$\begin{Bmatrix} M_{xx} \\ M_{yy} \\ M_{xy} \end{Bmatrix} = \int_{-\frac{h}{2}}^{+\frac{h}{2}} \begin{Bmatrix} \sigma_{xx} \\ \sigma_{yy} \\ \tau_{xy} \end{Bmatrix} z dz \tag{20}$$

$$\begin{Bmatrix} Q_x \\ Q_y \end{Bmatrix} = K \int_{-\frac{h}{2}}^{+\frac{h}{2}} \begin{Bmatrix} \tau_{xz} \\ \tau_{yz} \end{Bmatrix} dz \tag{21}$$

$$\begin{Bmatrix} I_0 \\ I_1 \\ I_2 \end{Bmatrix} = \int_{-\frac{h}{2}}^{+\frac{h}{2}} \begin{Bmatrix} 1 \\ z \\ z^2 \end{Bmatrix} \rho(x,y) dz \tag{22}$$

Where K is so-called the shear stress correction factor and is equal to $5/6$.
Based on FSDT, the stress-strain relations are given by:

$$\begin{Bmatrix} \sigma_{xx} \\ \sigma_{yy} \\ \tau_{yz} \\ \tau_{xz} \\ \tau_{xy} \end{Bmatrix} = \begin{bmatrix} Q_{11}(x,y) & Q_{12}(x,y) & 0 & 0 & 0 \\ Q_{12}(x,y) & Q_{22}(x,y) & 0 & 0 & 0 \\ 0 & 0 & Q_{44}(x,y) & 0 & 0 \\ 0 & 0 & 0 & Q_{55}(x,y) & 0 \\ 0 & 0 & 0 & 0 & Q_{66}(x,y) \end{bmatrix} \begin{Bmatrix} \varepsilon_{xx} \\ \varepsilon_{yy} \\ \gamma_{yz} \\ \gamma_{xz} \\ \gamma_{xy} \end{Bmatrix} \tag{23}$$

Where stiffness coefficients Q_{ij} are defined as:

$$Q_{11}(x,y) = Q_{22}(x,y) = \frac{E(x,y)}{1-\nu^2} \tag{24}$$

$$Q_{12}(x,y) = \frac{E(x,y)\nu}{1-\nu^2} \tag{25}$$

$$Q_{44}(x,y) = Q_{55}(x,y) = Q_{66}(x,y) = \frac{E(x,y)}{2(1+\nu)} \tag{26}$$

The Poisson ratio υ in the above relations is constant and equal to 0.3.
By relieving $(\delta u_0, \delta v_0, \delta w_0)$ of Eq. (18) using integration by parts and setting the coefficients of $(\delta u_0, \delta v_0, \delta w_0)$ to zero separately (i.e., using the fundamental lemma of calculus of variations), the General form of equations of motion for 2D-FG rectangular plate in the framework of the first-order shear deformation theory will be obtained:

$$\frac{\partial N_{xx}}{\partial x} + \frac{\partial N_{xy}}{\partial y} = I_0 \frac{\partial^2 u_0}{\partial t^2} + I_1 \frac{\partial^2 \phi_x}{\partial t^2} \tag{27}$$

$$\frac{\partial N_{yy}}{\partial y} + \frac{\partial N_{xy}}{\partial x} = I_0 \frac{\partial^2 v_0}{\partial t^2} + I_1 \frac{\partial^2 \phi_y}{\partial t^2} \tag{28}$$

$$\frac{\partial Q_x}{\partial x} + \frac{\partial Q_y}{\partial y} + \mathcal{N}(w_0) = I_0 \frac{\partial^2 w_0}{\partial t^2} \tag{29}$$

$$\frac{\partial M_{xx}}{\partial x} + \frac{\partial M_{xy}}{\partial y} - Q_x = I_1 \frac{\partial^2 u_0}{\partial t^2} + I_2 \frac{\partial^2 \phi_x}{\partial t^2} \tag{30}$$

$$\frac{\partial M_{yy}}{\partial y} + \frac{\partial M_{xy}}{\partial x} - Q_y = I_1 \frac{\partial^2 v_0}{\partial t^2} + I_2 \frac{\partial^2 \phi_y}{\partial t^2} \tag{31}$$

$\mathcal{N}(w_0)$ is:

$$\mathcal{N}(w_0) = \frac{\partial}{\partial x}\left(N_{xx}\frac{\partial w_0}{\partial x} + N_{xy}\frac{\partial w_0}{\partial y}\right) + \frac{\partial}{\partial y}\left(N_{yy}\frac{\partial w_0}{\partial y} + N_{xy}\frac{\partial w_0}{\partial x}\right) \tag{32}$$

In-plane inertia effects and rotary inertia effects can be ignored due to the thinness of the plate [51]. As a result, the Eqs. (27)-(31) reduce to:

$$\frac{\partial N_{xx}}{\partial x} + \frac{\partial N_{xy}}{\partial y} = 0 \tag{33}$$

$$\frac{\partial N_{yy}}{\partial y}+\frac{\partial N_{xy}}{\partial x}=0 \tag{34}$$

$$\frac{\partial Q_x}{\partial x}+\frac{\partial Q_y}{\partial y}+\mathcal{N}(w_0)=I_0\frac{\partial^2 w_0}{\partial t^2} \tag{35}$$

$$\frac{\partial M_{xx}}{\partial x}+\frac{\partial M_{xy}}{\partial y}-Q_x=0 \tag{36}$$

$$\frac{\partial M_{yy}}{\partial y}+\frac{\partial M_{xy}}{\partial x}-Q_y=0 \tag{37}$$

By replacing Eq. (23) into Eq. (19)-(22) and substituting the results into the Eq. (33)-(37), equations of motion can be written in terms of displacements:

(38)

$$\begin{aligned}
&2Q_{12}(x,y)\frac{\partial^2 \mathrm{v}(x,y,t)}{\partial x\,\partial y}+2Q_{66}(x,y)\frac{\partial^2 \mathrm{v}(x,y,t)}{\partial x\,\partial y}+2Q_{12}(x,y)\frac{\partial \mathrm{w}(x,y,t)}{\partial y}\frac{\partial^2 \mathrm{w}(x,y,t)}{\partial x\,\partial y}+\\
&2Q_{66}(x,y)\frac{\partial \mathrm{w}(x,y,t)}{\partial y}\frac{\partial^2 \mathrm{w}(x,y,t)}{\partial x\,\partial y}+2Q_{11}(x,y)\frac{\partial^2 \mathrm{u}(x,y,t)}{\partial x^2}+2Q_{66}(x,y)\frac{\partial^2 \mathrm{u}(x,y,t)}{\partial y^2}\\
&+2\frac{\partial Q_{11}(x,y)}{\partial x}\frac{\partial \mathrm{u}(x,y,t)}{\partial x}+2\frac{\partial Q_{66}(x,y)}{\partial y}\frac{\partial \mathrm{u}(x,y,t)}{\partial y}+2\frac{\partial Q_{12}(x,y)}{\partial x}\frac{\partial \mathrm{v}(x,y,t)}{\partial y}\\
&+2\frac{\partial Q_{66}(x,y)}{\partial y}\frac{\partial \mathrm{v}(x,y,t)}{\partial x}+2Q_{11}(x,y)\frac{\partial^2 \mathrm{w}(x,y,t)}{\partial x^2}\frac{\partial \mathrm{w}(x,y,t)}{\partial x}\\
&+2Q_{66}(x,y)\frac{\partial^2 \mathrm{w}(x,y,t)}{\partial y^2}\frac{\partial \mathrm{w}(x,y,t)}{\partial x}+\frac{\partial Q_{11}(x,y)}{\partial x}\left(\frac{\partial \mathrm{w}(x,y,t)}{\partial x}\right)^2\\
&+2\frac{\partial Q_{66}(x,y)}{\partial y}\frac{\partial w(x,y,t)}{\partial y}\frac{\partial w(x,y,t)}{\partial x}+\frac{\partial Q_{12}(x,y)}{\partial x}\left(\frac{\partial w(x,y,t)}{\partial y}\right)^2=0
\end{aligned}$$

$$\begin{aligned}
&2Q_{12}(x,y)\frac{\partial^2 \mathrm{u}(x,y,t)}{\partial x\,\partial y}+2Q_{66}(x,y)\frac{\partial^2 \mathrm{u}(x,y,t)}{\partial x\,\partial y}+2Q_{12}(x,y)\frac{\partial \mathrm{w}(x,y,t)}{\partial x}\frac{\partial^2 \mathrm{w}(x,y,t)}{\partial x\,\partial y}+\\
&2Q_{66}(x,y)\frac{\partial \mathrm{w}(x,y,t)}{\partial x}\frac{\partial^2 \mathrm{w}(x,y,t)}{\partial x\,\partial y}+2\frac{\partial Q_{12}(x,y)}{\partial y}\frac{\partial \mathrm{u}(x,y,t)}{\partial x}+2\frac{\partial Q_{66}(x,y)}{\partial x}\frac{\partial \mathrm{u}(x,y,t)}{\partial y}\\
&+2Q_{66}(x,y)\frac{\partial^2 \mathrm{v}(x,y,t)}{\partial x^2}+2Q_{22}(x,y)\frac{\partial^2 \mathrm{v}(x,y,t)}{\partial y^2}+2\frac{\partial Q_{22}(x,y)}{\partial y}\frac{\partial \mathrm{v}(x,y,t)}{\partial y}\\
&+2\frac{\partial Q_{66}(x,y)}{\partial x}\frac{\partial \mathrm{v}(x,y,t)}{\partial x}+2Q_{66}(x,y)\frac{\partial \mathrm{w}(x,y,t)}{\partial y}\frac{\partial^2 \mathrm{w}(x,y,t)}{\partial x^2}\\
&+2Q_{22}(x,y)\frac{\partial w(x,y,t)}{\partial y}\frac{\partial^2 w(x,y,t)}{\partial y^2}+\frac{\partial Q_{12}(x,y)}{\partial y}\left(\frac{\partial w(x,y,t)}{\partial x}\right)^2\\
&+2\frac{\partial Q_{66}(x,y)}{\partial x}\frac{\partial w(x,y,t)}{\partial y}\frac{\partial w(x,y,t)}{\partial x}+\frac{\partial Q_{22}(x,y)}{\partial y}\left(\frac{\partial w(x,y,t)}{\partial y}\right)^2=0
\end{aligned} \tag{39}$$

$$\begin{aligned}
&\frac{\partial Q_{11}(x,y)}{\partial x}\left(\frac{\partial \mathrm{w}(x,y,t)}{\partial x}\right)^3+\frac{\partial \mathrm{w}(x,y,t)}{\partial y}\frac{\partial Q_{12}(x,y)}{\partial y}\left(\frac{\partial \mathrm{w}(x,y,t)}{\partial x}\right)^2\\
&+2\frac{\partial \mathrm{w}(x,y,t)}{\partial y}\frac{\partial Q_{66}(x,y)}{\partial y}\left(\frac{\partial \mathrm{w}(x,y,t)}{\partial x}\right)^2+3\frac{\partial^2 \mathrm{w}(x,y,t)}{\partial x^2}Q_{11}(x,y)\left(\frac{\partial \mathrm{w}(x,y,t)}{\partial x}\right)^2\\
&+\frac{\partial^2 \mathrm{w}(x,y,t)}{\partial y^2}Q_{12}(x,y)\left(\frac{\partial \mathrm{w}(x,y,t)}{\partial x}\right)^2+2\frac{\partial^2 \mathrm{w}(x,y,t)}{\partial y^2}Q_{66}(x,y)\left(\frac{\partial \mathrm{w}(x,y,t)}{\partial x}\right)^2\\
&+2\frac{\partial \mathrm{u}(x,y,t)}{\partial x}\frac{\partial Q_{11}(x,y)}{\partial x}\frac{\partial \mathrm{w}(x,y,t)}{\partial x}+\left(\frac{\partial \mathrm{w}(x,y,t)}{\partial y}\right)^2\frac{\partial Q_{12}(x,y)}{\partial x}\frac{\partial \mathrm{w}(x,y,t)}{\partial x}+
\end{aligned} \tag{40}$$

$$2\frac{\partial \mathrm{v}(x,y,t)}{\partial y}\frac{\partial Q_{12}(x,y)}{\partial x}\frac{\partial \mathrm{w}(x,y,t)}{\partial x}+2\frac{\partial Q_{55}(x,y)}{\partial x}\frac{\partial \mathrm{w}(x,y,t)}{\partial x}+$$
$$2\left(\frac{\partial \mathrm{w}(x,y,t)}{\partial y}\right)^2\frac{\partial Q_{66}(x,y)}{\partial x}\frac{\partial \mathrm{w}(x,y,t)}{\partial x}+2\frac{\partial \mathrm{u}(x,y,t)}{\partial y}\frac{\partial Q_{66}(x,y)}{\partial y}\frac{\partial \mathrm{w}(x,y,t)}{\partial x}+$$
$$2\frac{\partial \mathrm{v}(x,y,t)}{\partial x}\frac{\partial Q_{66}(x,y)}{\partial y}\frac{\partial \mathrm{w}(x,y,t)}{\partial x}+2\frac{\partial^2 \mathrm{u}(x,y,t)}{\partial x^2}Q_{11}(x,y)\frac{\partial \mathrm{w}(x,y,t)}{\partial x}+$$
$$2\frac{\partial^2 \mathrm{v}(x,y,t)}{\partial x\,\partial y}Q_{12}(x,y)\frac{\partial \mathrm{w}(x,y,t)}{\partial x}+4\frac{\partial \mathrm{w}(x,y,t)}{\partial y}\frac{\partial^2 \mathrm{w}(x,y,t)}{\partial x\,\partial y}Q_{12}(x,y)\frac{\partial \mathrm{w}(x,y,t)}{\partial x}+$$
$$2\frac{\partial^2 \mathrm{u}(x,y,t)}{\partial y^2}Q_{66}(x,y)\frac{\partial \mathrm{w}(x,y,t)}{\partial x}+2\frac{\partial^2 \mathrm{v}(x,y,t)}{\partial x\,\partial y}Q_{66}(x,y)\frac{\partial \mathrm{w}(x,y,t)}{\partial x}+$$
$$8\frac{\partial \mathrm{w}(x,y,t)}{\partial y}\frac{\partial^2 \mathrm{w}(x,y,t)}{\partial x\,\partial y}Q_{66}(x,y)\frac{\partial \mathrm{w}(x,y,t)}{\partial x}+2\frac{\partial \mathrm{u}(x,y,t)}{\partial x}\frac{\partial \mathrm{w}(x,y,t)}{\partial y}\frac{\partial Q_{12}(x,y)}{\partial y}+$$
$$\left(\frac{\partial \mathrm{w}(x,y,t)}{\partial y}\right)^3\frac{\partial Q_{22}(x,y)}{\partial y}+2\frac{\partial \mathrm{v}(x,y,t)}{\partial y}\frac{\partial \mathrm{w}(x,y,t)}{\partial y}\frac{\partial Q_{22}(x,y)}{\partial y}+2\frac{\partial \mathrm{w}(x,y,t)}{\partial y}\frac{\partial Q_{44}(x,y)}{\partial y}$$
$$+2\frac{\partial \mathrm{u}(x,y,t)}{\partial y}\frac{\partial \mathrm{w}(x,y,t)}{\partial y}\frac{\partial Q_{66}(x,y)}{\partial x}+2\frac{\partial \mathrm{v}(x,y,t)}{\partial x}\frac{\partial \mathrm{w}(x,y,t)}{\partial y}\frac{\partial Q_{66}(x,y)}{\partial x}$$
$$+2\frac{\partial \mathrm{u}(x,y,t)}{\partial x}\frac{\partial^2 \mathrm{w}(x,y,t)}{\partial x^2}Q_{11}(x,y)+\left(\frac{\partial \mathrm{w}(x,y,t)}{\partial y}\right)^2\frac{\partial^2 \mathrm{w}(x,y,t)}{\partial x^2}Q_{12}(x,y)+$$
$$2\frac{\partial \mathrm{v}(x,y,t)}{\partial y}\frac{\partial^2 \mathrm{w}(x,y,t)}{\partial x^2}Q_{12}(x,y)+2\frac{\partial \mathrm{u}(x,y,t)}{\partial x}\frac{\partial^2 \mathrm{w}(x,y,t)}{\partial y^2}Q_{12}(x,y)+$$
$$2\frac{\partial \mathrm{w}(x,y,t)}{\partial y}\frac{\partial^2 \mathrm{u}(x,y,t)}{\partial x\,\partial y}Q_{12}(x,y)+2\frac{\partial^2 \mathrm{v}(x,y,t)}{\partial y^2}\frac{\partial \mathrm{w}(x,y,t)}{\partial y}Q_{22}(x,y)+$$
$$3\left(\frac{\partial \mathrm{w}(x,y,t)}{\partial y}\right)^2\frac{\partial^2 \mathrm{w}(x,y,t)}{\partial y^2}Q_{22}(x,y)+2\frac{\partial \mathrm{v}(x,y,t)}{\partial y}\frac{\partial^2 \mathrm{w}(x,y,t)}{\partial y^2}Q_{22}(x,y)+$$
$$2\frac{\partial^2 \mathrm{w}(x,y,t)}{\partial y^2}Q_{44}(x,y)+2\frac{\partial \phi_Y(x,y,t)}{\partial y}Q_{44}(x,y)+2\frac{\partial^2 \mathrm{w}(x,y,t)}{\partial x^2}Q_{55}(x,y)+$$
$$2\frac{\partial \phi_X(x,y,t)}{\partial x}Q_{55}(x,y)+2\frac{\partial^2 \mathrm{v}(x,y,t)}{\partial x^2}\frac{\partial \mathrm{w}(x,y,t)}{\partial y}Q_{66}(x,y)$$
$$+2\left(\frac{\partial \mathrm{w}(x,y,t)}{\partial y}\right)^2\frac{\partial^2 \mathrm{w}(x,y,t)}{\partial x^2}Q_{66}(x,y)+2\frac{\partial \mathrm{w}(x,y,t)}{\partial y}\frac{\partial^2 \mathrm{u}(x,y,t)}{\partial x\,\partial y}Q_{66}(x,y)+$$
$$4\frac{\partial \mathrm{u}(x,y,t)}{\partial y}\frac{\partial^2 \mathrm{w}(x,y,t)}{\partial x\,\partial y}Q_{66}(x,y)+4\frac{\partial \mathrm{v}(x,y,t)}{\partial x}\frac{\partial^2 \mathrm{w}(x,y,t)}{\partial x\,\partial y}Q_{66}(x,y)+$$
$$2\frac{\partial Q_{55}(x,y)}{\partial x}\phi_X(x,y,t)+2\frac{\partial Q_{44}(x,y)}{\partial y}\phi_Y(x,y,t)-2\frac{\partial^2 \mathrm{w}(x,y,t)}{\partial t^2}\rho(x,y)=0$$

$$h^2Q_{12}(x,y)\frac{\partial^2\phi_Y(x,y,t)}{\partial x\,\partial y}+h^2Q_{66}(x,y)\frac{\partial^2\phi_Y(x,y,t)}{\partial x\,\partial y}+h^2Q_{11}(x,y)\frac{\partial^2\phi_X(x,y,t)}{\partial x^2}+h^2Q_{66}(x,y)\frac{\partial^2\phi_X(x,y,t)}{\partial y^2}+h^2\frac{\partial Q_{11}(x,y)}{\partial x}\frac{\partial\phi_X(x,y,t)}{\partial x}+h^2\frac{\partial Q_{66}(x,y)}{\partial y}\frac{\partial\phi_X(x,y,t)}{\partial y}+h^2\frac{\partial Q_{66}(x,y)}{\partial y}\frac{\partial\phi_Y(x,y,t)}{\partial x}+h^2\frac{\partial Q_{12}(x,y)}{\partial x}\frac{\partial\phi_Y(x,y,t)}{\partial y}-12Q_{55}(x,y)\frac{\partial w(x,y,t)}{\partial x}-12Q_{55}(x,y)\phi_X(x,y,t)=0 \quad (41)$$

$$h^2Q_{12}(x,y)\frac{\partial^2\phi_X(x,y,t)}{\partial x\,\partial y}+h^2Q_{66}(x,y)\frac{\partial^2\phi_X(x,y,t)}{\partial x\,\partial y}+h^2Q_{66}(x,y)\frac{\partial^2\phi_Y(x,y,t)}{\partial x^2}+h^2\frac{\partial Q_{12}(x,y)}{\partial y}\frac{\partial\phi_X(x,y,t)}{\partial x}+h^2\frac{\partial Q_{66}(x,y)}{\partial x}\frac{\partial\phi_X(x,y,t)}{\partial y}+h^2Q_{22}(x,y)\frac{\partial^2\phi_Y(x,y,t)}{\partial y^2}+h^2\frac{\partial Q_{66}(x,y)}{\partial x}\frac{\partial\phi_Y(x,y,t)}{\partial x}+h^2\frac{\partial Q_{22}(x,y)}{\partial y}\frac{\partial\phi_Y(x,y,t)}{\partial y}-12Q_{44}(x,y)\frac{\partial w(x,y,t)}{\partial y}-12Q_{44}(x,y)\phi_Y(x,y,t)=0 \quad (42)$$

The following boundary conditions for simply supported plate according to the FSDT are considered:

$$at\ \ x = 0, a \qquad v_0 = w_0 = N_{xx} = M_{xx} = \phi_y = 0 \tag{43}$$

$$at\ \ y = 0, b \qquad u_0 = w_0 = N_{yy} = M_{yy} = \phi_x = 0 \tag{44}$$

The boundary conditions in Eq. (43) and (44) are satisfied by the following admissible functions [52]:

$$u_0(x,y,t) = \sum_{p=1}^{\infty}\sum_{q=1}^{\infty} U_{pq}(t)\cos(\alpha x)\sin(\beta y) \tag{45}$$

$$v_0(x,y,t) = \sum_{p=1}^{\infty}\sum_{q=1}^{\infty} V_{pq}(t)\sin(\alpha x)\cos(\beta y) \tag{46}$$

$$w_0(x,y,t) = \sum_{p=1}^{\infty}\sum_{q=1}^{\infty} W_{pq}(t)\sin(\alpha x)\sin(\beta y) \tag{47}$$

$$\phi_x(x,y,t) = \sum_{p=1}^{\infty}\sum_{q=1}^{\infty} X_{pq}(t)\cos(\alpha x)\sin(\beta y) \tag{48}$$

$$\phi_y(x,y,t) = \sum_{p=1}^{\infty}\sum_{q=1}^{\infty} Y_{pq}(t)\sin(\alpha x)\cos(\beta y) \tag{49}$$

Where $\alpha = \frac{q\pi}{a}$ and $\beta = \frac{p\pi}{b}$, and p and q are the half-wave numbers.
For the simplification, a set of dimensionless parameters are introduced as:

$$(\bar{u},\bar{v},\bar{w}) = \frac{(u,v,w)}{h} \quad (\bar{x},\bar{y}) = \left(\frac{x}{a},\frac{y}{b}\right) \quad (r,s) = \left(\frac{a}{b},\frac{a}{h}\right) \quad \bar{E} = \frac{E}{E_m} \quad \bar{\rho} = \frac{\rho}{\rho_m} \quad \tau = \frac{t}{h}\sqrt{\frac{E_m}{\rho_m}} \tag{50}$$

Considering only one term in the Eq. (45)-(49) and by replacing they into Eq. (38)-(42) and then applying Galerkin method the time dependent nonlinear differential equations of motion after applying dimensionless parameters and some mathematical simplifications can be derived as:

$$C_{11}\bar{W}^2 + C_{12}\bar{U} + C_{13}\bar{V} = 0 \tag{51}$$

$$C_{21}\bar{W}^2 + C_{22}U + C_{23}V = 0 \tag{52}$$

$$C_{31}\frac{d^2\bar{W}}{d\tau^2} + C_{32}\bar{W} + C_{33}\bar{U}\bar{W} + C_{34}\bar{V}\bar{W} + C_{35}\bar{W}^3 + C_{36}X + C_{37}Y = 0 \tag{53}$$

$$C_{41}\bar{W} + C_{42}X + C_{43}Y = 0 \tag{54}$$

$$C_{51}\bar{W} + C_{52}X + C_{53}Y = 0 \tag{55}$$

Where C_{ij} are non-dimensional coefficients that are related to the dimensions and plate properties and are presented in Appendix A. By substituting $U, V, X,$ and Y in terms of $W(t)$ obtained from the Eq. (51), (52), (54), and (55), into the Eq. (53) results in the nonlinear time-dependent equation in $W(t)$:

$$\frac{d^2\bar{W}}{d\tau^2} + \alpha\,\bar{W} + \gamma\,\bar{W}^3 = 0 \tag{56}$$

Where the coefficients α and γ' are given in Appendix B.

4 Solution method

In the present research, Modified Lindstedt-Poincare method is used to solve Eq. (56). The assumed initial condition is expressed as:

$$\bar{W}(0) = \frac{W_{max}}{h} = A \qquad \frac{d\bar{W}(0)}{d\tau} = 0 \tag{57}$$

Where A is the non-dimensional maximum vibration amplitude. For the necessity of proposed method, a positive, dimensionless and small parameter must be defined. Therefore Eq. (56) should be rewritten as follows:

$$\frac{d^2\bar{W}}{d\tau^2} + \alpha\,\bar{W} + \epsilon\frac{a\,\gamma}{h}\,\bar{W}^3 = 0 \tag{58}$$

Where ϵ is bookkeeping parameter and is defined as follows:

$$\epsilon = \frac{h}{a} \tag{59}$$

Linear frequency of FG plate from Eq. (58) is:

$$\alpha = \omega_l^2 \tag{60}$$

According to the References [53, 54], $\bar{W}(\tau)$ and α can be written as a series in ϵ:

$$\bar{W} = \bar{W}_0 + \epsilon\,\bar{W}_1 + \epsilon^2\bar{W}_2 + \cdots \tag{61}$$

$$\alpha = \omega_{NL}^2 + \epsilon\,c_1 + \epsilon^2 c_2 + \cdots \tag{62}$$

Where nonlinear frequency ω_{NL} and $c_1, c_2, \ldots and\ c_i$ (for $i = 1, \ldots, \infty$) are unknown coefficients which are calculated in next section.

By Substituting Eq. (61) and (62) into Eq. (58), and then equating coefficients $\epsilon^0, \epsilon^1\ and\ \epsilon^2$ to zero, yields the following equations:

$$\epsilon^0: \quad \ddot{\bar{W}}_0 + \omega^2\bar{W}_0 = 0 \qquad \bar{W}_0(0) = A \qquad \frac{d\bar{W}_0}{d\tau}(0) = 0 \tag{63}$$

$$\epsilon^1: \quad \ddot{\bar{W}}_1 + \omega^2\bar{W}_1 = -c_1\bar{W}_0 - \beta\bar{W}_0^2 - \gamma\bar{W}_0^3 \qquad \bar{W}_1(0) = 0 \qquad \frac{d\bar{W}_1}{d\tau}(0) = 0 \tag{64}$$

$$\epsilon^2: \quad \ddot{\bar{W}}_2 + \omega^2\bar{W}_2 = -c_2\bar{W}_0 - c_1\bar{W}_1 - 2\beta\bar{W}_0\bar{W}_1 - 3\gamma\bar{W}_1\bar{W}_0^2 \qquad \bar{W}_2(0) = 0 \qquad \frac{d\bar{W}_2}{d\tau}(0) = 0 \tag{65}$$

The result of solving Eq. (63) with the corresponding initial condition is as follow:

$$\bar{W}_0 = A\cos(\omega\tau) \tag{66}$$

Substituting Eq. (66) into Eq. (64) gives:

$$\ddot{\bar{W}}_1 + \omega^2\bar{W}_1 = \left(-c_1 A - \frac{3}{4}\gamma A^3\right)\cos(\omega\tau) - \frac{1}{2}\beta A^2\cos(2\omega\tau) \tag{67}$$

In order to have a periodic response for $\bar{W}_1$, secular term must eliminate in Eq. (67). So:

$$c_1 = -\frac{3}{4}\gamma A^2 \tag{68}$$

The solution of Eq. (67) is:

$$\bar{W}_1 = \left(\frac{\beta A^2}{3\omega^2} - \frac{\gamma A^3}{32\omega^2}\right)\cos(\omega\tau) + \frac{\beta A^2}{6\omega^2}\cos(2\omega\tau) + \frac{\gamma A^3}{32\omega^2}\cos(3\omega\tau) - \frac{\beta A^2}{2\omega^2} \tag{69}$$

Similarly, by substituting Eqs. (66) and (69) into Eq. (65) and avoiding the secular term, unknown coefficient c_2 is obtained:

$$c_2 = \frac{\beta\gamma A^3}{4\omega^2} - \frac{3\gamma^2 A^4}{128\omega^2} + \frac{5\beta^2 A^2}{6\omega^2} - \frac{3\beta\gamma A^3}{4\omega^2} + \frac{3\gamma^2 A^4}{64\omega^2} \tag{70}$$

Eq. (62), (68), and (70) give the nonlinear natural frequency, that is:

$$\omega_{NL} = \sqrt{\frac{\left(\alpha + \frac{3}{4}\gamma\epsilon A^2\right) + \sqrt{\left(\alpha + \frac{3}{4}\epsilon\gamma A^2\right)^2 + \left(2\beta\gamma A^3 - \frac{10\beta^2 A^2}{3} - \frac{3\gamma^2 A^4}{32}\right)\epsilon^2}}{2}} \tag{71}$$

After solving Eq. (65), $\bar{W}_2$ is obtained to be:

$$\begin{aligned}\bar{W}_2 = &\left(\frac{c_1\beta A^2}{2\omega^4} - \frac{\beta^2 A^3}{3\omega^4} + \frac{21\beta\gamma A^4}{32\omega^4}\right) \\ &+ \left(-\frac{5c_1\beta A^2}{9\omega^4} - \frac{c_1\gamma A^3}{256\omega^4} + \frac{61\beta^2 A^3}{144\omega^4} - \frac{17\beta\gamma A^4}{32\omega^4} - \frac{\gamma^2 A^5}{256\omega^4}\right)cos(\omega\tau) \\ &+ \left(\frac{c_1\beta A^2}{18\omega^2} - \frac{\beta^2 A^3}{9\omega^2} - \frac{\beta\gamma A^4}{6\omega^2}\right)cos(2\omega\tau) \\ &+ \left(\frac{c_1\gamma A^3}{256\omega^2} + \frac{\beta^2 A^3}{48\omega^2} + \frac{\beta\gamma A^4}{32\omega^2} + \frac{3\gamma^2 A^5}{1024\omega^2}\right)cos(3\omega\tau) + \left(\frac{\beta\gamma A^4}{96\omega^2}\right)cos(4\omega\tau) \\ &+ \left(\frac{\gamma^2 A^5}{1024\omega^2}\right)cos(5\omega\tau)\end{aligned} \tag{72}$$

Eventually, the second order approximation of the solution become as follows:

$$\bar{W}_{2nd} = \bar{W}_0 + \epsilon\,\bar{W}_1 + \epsilon^2\,\bar{W}_2 \tag{73}$$

5 Comparison study

In this section, to examine the accuracy and efficiency of the present formulation, the results of this paper are compared with the existing data available in previously published papers.

As the first comparison study, frequency parameters $\beta = \omega h\sqrt{\frac{\rho_c}{E_c}}$ of simply supported FG square plates are given in Table (2), for different values of length to thickness ratio and power law exponent. Included in this table are also the results of the exact solutions of FG rectangular plates based on the first and third-order shear deformation plate theory reported by Hosseini Hashemi et al. [10], element-free kp-Ritz method obtained by Zhao et al [11]. It is clearly evident that the excellent agreements are found between the results.

As seen in the previous section, the nonlinear equation of transverse motion for 2D-FG rectangular plate is solved analytically by the modified Lindstedt-Poincare method. In order to ensure the accuracy and convergence of this solution approach, the nonlinear to linear frequency ratio of FG rectangular plate based on first order shear deformation theory is obtained and then compared with the results given by Yazdi [15]. From Table (3), there is little difference between present results and Yazdi [15]. The reason for this difference is that the shear effects are ignored in the reference [15]. In other words, the results of the present study are more accurate than the reference [15].

Table 2 Comparison of fundamental frequency parameter $\boldsymbol{\beta = \omega h\sqrt{\frac{\rho_c}{E_c}}}$ for $\boldsymbol{Al/Al_2O_3}$ square plates

References	$\frac{a}{h}$	n 0	0.5	1	4	10
[10]	20	0.0148	0.0128	0.0115	0.0101	0.0096
[11]		0.0146	0.0124	0.0112	0.0097	0.0093
Present study		0.0148	0.0126	0.0113	0.0098	0.0094
[10]	10	0.0577	0.0492	0.0445	0.0383	0.0363
[11]		0.0567	0.0482	0.0435	0.0376	0.0359
Present study		0.0581	0.0494	0.0445	0.386	0.0369
[10]	5	0.2112	0.1806	0.1650	0.1371	0.1304
[11]		0.2055	0.1757	0.1587	0.1356	0.1284
Present study		0.2158	0.1847	0.1672	0.1435	0.1356

6 Results and discussion

In this section, the influences of some key plate parameters such as dimensionless vibration amplitude (A), aspect ratio $\left(\frac{a}{b}\right)$, width FG index (m) and length FG index (n) on the nonlinear frequency ratio $\left(\frac{\omega_{NL}}{\omega_L}\right)$ of 2D-FG rectangular plate are presented in tabular and graphical forms. The results are reported for plate which is made of a mixture of aluminum (Al) and alumina (Al_2O_3) in which their material properties are listed in Table (1). It should be note that the nonlinear frequency ratio is described as the ratio of nonlinear natural frequency to linear natural frequency in all cases in this section.

Table (4) provided the effects of dimensionless vibration amplitude (A) on the nonlinear frequency ratio $\left(\frac{\omega_{NL}}{\omega_L}\right)$ of 2D-FG rectangular plate for different volume fraction indexes m and n. The numerical results are performed for aspect ratio $\frac{a}{b} = 1$ and length to thickness ratio $\frac{a}{h} = 20$.

This table shows that higher dimensionless vibration amplitude results in a larger nonlinear frequency ratio for different volume fraction indexes. In other word, the discrepancy between nonlinear and linear frequency is deeply depend on the vibration amplitude.

Table (5) shows the effects of length-thickness ratio $\frac{a}{h}$ on nonlinear frequency ratio of 2D-FG square plate for different values of volume fraction indexes with $A = 1$. It can be seen from Table 5, the nonlinear frequencies ratio of the of 2D-FG square plate will enlarge with the decreasing of length-thickness ratio. This is due to as $\frac{a}{h}$ increases, the plate becomes more flexible and hence its effective stiffness reduces. It is implied that the 2D FG plate with a higher length-thickness ratio has a lower nonlinear frequency. Figure (2) shows the variation of the nonlinear frequency versus width FG index (m) for different values of length FG index (n) when $A = 1$ and $\frac{a}{h} = 20$. As seen from the figure, nonlinear frequency decreases on increasing width FG index.

Table 3 Comparison of nonlinear to linear frequency ratio for square FG plate ($\frac{a}{h} = 40$)

	$n = 0.2$		$n = 10$	
$\frac{W_{max}}{h}$	FSDT	CPT [15]	FSDT	CPT [15]
0.25	1.0529	1.0467	1.0473	1.0413
0.5	1.1962	1.1758	1.1766	1.1563
0.75	1.4005	1.3641	1.3630	1.3266
1.0	1.6428	1.5911	1.5860	1.5335
1.25	1.9086	1.8426	1.8323	1.7645
1.5	2.1895	2.1103	2.0937	2.0115
1.75	2.4805	2.3890	2.3654	2.2996
2	2.7785	2.6755	2.6442	2.5355

Table 4 Nonlinear frequency ratio for 2D-FG square plate ($\frac{a}{h} = 20$)

A		m				
	n	0	1	2	5	10
0.25	0	1.0597	1.0597	1.0666	1.0812	1.0905
	1	1.0597	1.0597	1.0646	1.0725	1.0766
	2	1.0629	1.0619	1.0632	1.0656	1.0677
	5	1.0701	1.0656	1.0620	1.0590	1.0594
	10	1.0732	1.0669	1.0622	1.0583	1.0582
0.75	0	1.4449	1.4449	1.4888	1.5784	1.6333
	1	1.4449	1.4449	1.4757	1.5254	1.5504
	2	1.4654	1.4590	1.4672	1.4823	1.4953
	5	1.5108	1.4826	1.4595	1.4401	1.4430
	10	1.5299	1.4903	1.4609	1.4354	1.4347
1.25	0	1.9976	1.9976	2.0846	2.2592	2.3646
	1	1.9976	1.9976	2.0587	2.1564	2.2051
	2	2.0383	2.0257	2.0418	2.0718	2.0974
	5	2.1277	2.0723	2.0267	1.9881	1.9938
	10	2.1651	2.0875	2.0293	1.9786	1.9772
1.75	0	2.6139	2.6139	2.7436	3.0020	3.1569
	1	2.6139	2.6139	2.7051	2.8501	2.9222
	2	2.6748	2.6560	2.6800	2.7247	2.7627
	5	2.8077	2.7254	2.6575	2.5998	2.6083
	10	2.8631	2.7480	2.6614	2.5856	2.5835
2.25	0	3.2586	3.2586	3.4302	3.7708	3.9744
	1	3.2586	3.2586	3.3792	3.5708	3.6657
	2	3.3391	3.3143	3.3461	3.4052	3.4553
	5	3.5148	3.4061	3.3162	3.2398	3.2511
	10	3.5879	3.4360	3.3214	3.2210	3.2181

Figure (3) shows the variation of the nonlinear frequency versus length FG index (n) for different values of width FG index (m) when $A = 1$ and $\frac{a}{h} = 20$. Results show that increasing the length FG index results in nonlinear frequency decreases. It follows from figures (2) and (3) that the nonlinear frequencies of the 2D-FG rectangular plates are strongly influenced by volume fraction indexes. In fact, the higher materials indexes mean the less volume fraction of ceramic phase in the 2D-FG plate, which induces more reduction in the total stiffness of the plate. Through the fact that a vibration frequency is directly proportional to the plate stiffness, e.g. Young's modulus, whilst it is inversely proportional to the plate mass one can be inferred

that by increasing volume fraction indexes, the nonlinear frequency decreases. Also From these figures it's conclude that smaller volume fraction indexes play a significant role in the nonlinear frequencies. Figures (4) and (5) are a backbone curve that exhibits effect of vibration amplitude on nonlinear frequency ratio of 2D-FG rectangular plate for different values of volume fraction indexes n and m when $\frac{a}{h} = 20$. As is clear from this figures, volume fraction indexes have noticeable effect on the nonlinear frequency ratio. By increasing the volume fraction indexes, backbone curves go away from vertical axis. In other word, by increasing volume fraction indexes, the degree of hardening nonlinearity behavior decreases. Moreover, it should be note that all response curves show initial softening type behavior, turning to hardening type for larger vibration amplitudes although the hardening degree is different.

Figure (6) describes the variation of the nonlinear frequency ratio with the aspect ratio for different values of length FG index (n) while total area of plate is constant when $A = 1$, $\frac{a}{h} = 20$ and $m = 0$. It is observed that for different n fast decreasing in nonlinear frequency ratio is obtained with an increase in aspect ratio for $\frac{a}{b} < 1.25$, while for $1.25 < \frac{a}{b}$, nonlinear frequency ratio is increased by increasing aspect ratio. Figure (7) depicts the variation of the nonlinear frequency ratio versus the aspect ratio for different values of width FG index (m) while total area of plate is constant when $A = 1$, $\frac{a}{h} = 20$ and $n = 0$. It is observed that for different m decreasing in nonlinear frequency ratio is obtained with an increase in aspect ratio for $\frac{a}{b} < 0.8$, while for $0.8 < \frac{a}{b}$, nonlinear frequency ratio is increased by increasing aspect ratio.

Table 5 Nonlinear frequency ratio for 2D-FG square plate ($\boldsymbol{A = 1}$)

$\frac{a}{h}$		m				
	n	0	1	2	5	10
5	0	1.8036	1.8036	1.8743	2.0203	2.1089
	1	1.8036	1.8036	1.8531	1.9339	1.9746
	2	1.8358	1.8257	1.8391	1.8653	1.8870
	5	1.9103	1.8637	1.8276	1.7982	1.8031
	10	1.9416	1.8764	1.8301	1.7904	1.7891
10	0	1.7286	1.7286	1.7951	1.9301	2.0121
	1	1.7286	1.7286	1.7752	1.8504	1.8881
	2	1.7595	1.7499	1.7623	1.7856	1.8054
	5	1.8284	1.7856	1.7509	1.7218	1.7263
	10	1.8573	1.7973	1.7530	1.7146	1.7135
20	0	1.7093	1.7093	1.7747	1.9069	1.9871
	1	1.7093	1.7093	1.7552	1.8289	1.8658
	2	1.7399	1.7305	1.7426	1.7651	1.7844
	5	1.8073	1.7655	1.7312	1.7022	1.7065
	10	1.8356	1.7770	1.7332	1.6951	1.6941
50	0	1.7039	1.7039	1.7690	1.9003	1.9801
	1	1.7039	1.7039	1.7496	1.8229	1.8595
	2	1.7344	1.7250	1.7370	1.7594	1.7785
	5	1.8013	1.7598	1.7256	1.6967	1.7010
	10	1.8294	1.7712	1.7276	1.6896	1.6886
100	0	1.7031	1.7031	1.7682	1.8993	1.9790
	1	1.7031	1.7031	1.7488	1.8220	1.8586
	2	1.7336	1.7242	1.7362	1.7585	1.7776
	5	1.8005	1.7590	1.7248	1.6959	1.7002
	10	1.8285	1.7704	1.7268	1.6888	1.6887

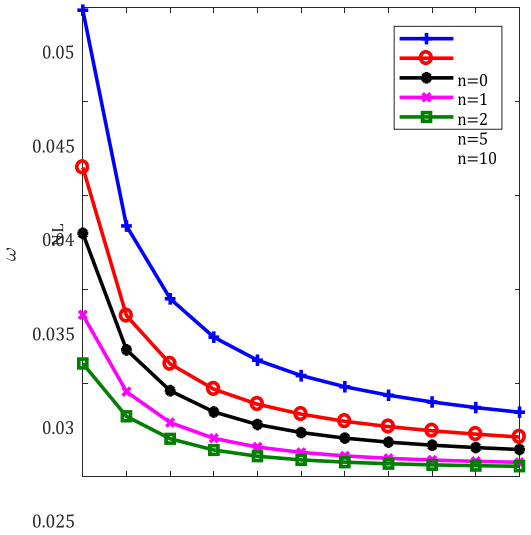

Figure 2 Variation of nonlinear frequency versus width FG index (m) for different values of n

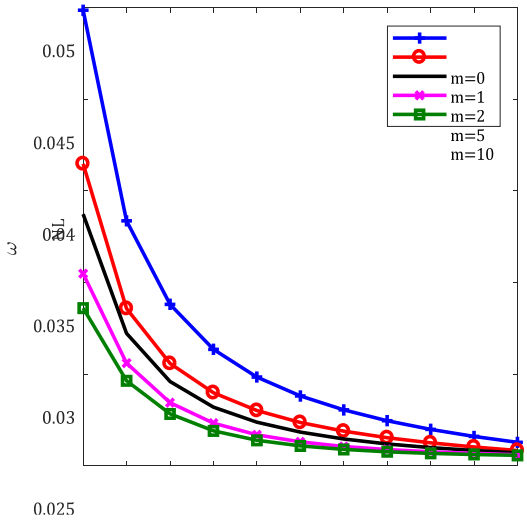

Figure 3 Variation of nonlinear frequency versus length FG index (n) for different values of m

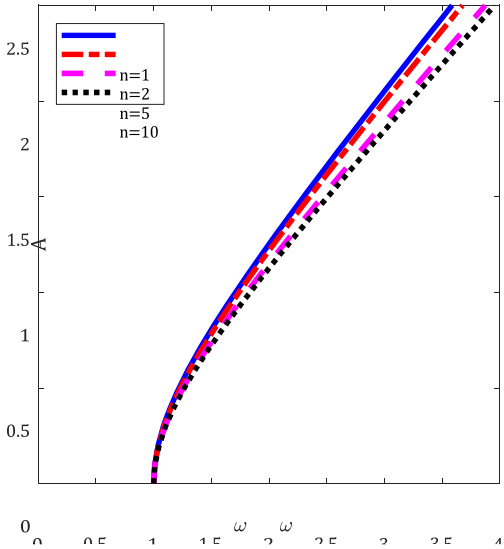

Figure 4 Effect of vibration amplitude on nonlinear frequency ratio for different values of volume fraction index n (m=0)

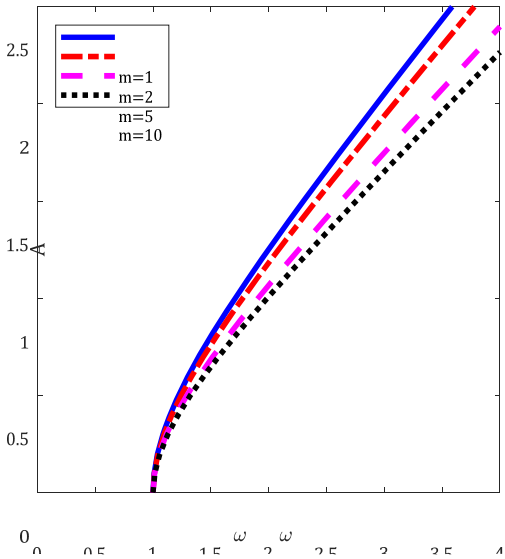

Figure 5 Effect of vibration amplitude on nonlinear frequency ratio for different values of volume fraction index m (n=0)

7 Conclusion

In this paper, the nonlinear free vibration analysis of 2D-FG rectangular plate are studied for the first time. For this purpose, the nonlinear partial differential motion equations are first developed based on FSDT and von Karman nonlinearity strain displacement relations. Then, nonlinear ordinary differential equations are obtained by applying Galerkin method. MLP method is used to obtain the analytical solution for the nonlinear vibrations of 2D-FG plate. The results are in good agreement with those obtained in previously published paper and numerical method. Finally, the effects of some key system parameters such as vibration amplitude, volume fraction indexes and aspect ratio on the nonlinear frequency are investigated.

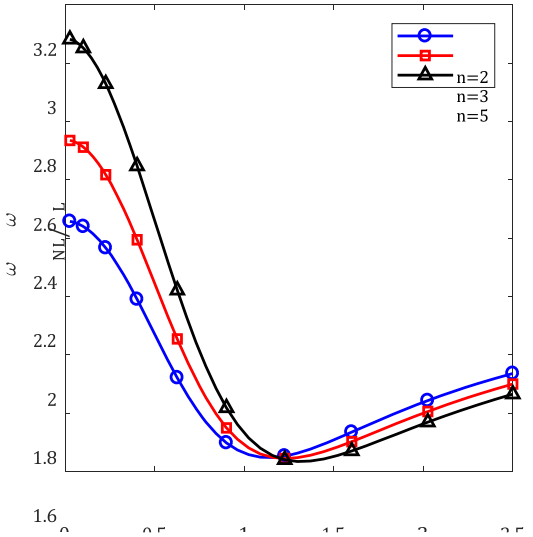

Figure 6 Aspect ratio effect on the nonlinear frequency ratio for different values of n (m=0)

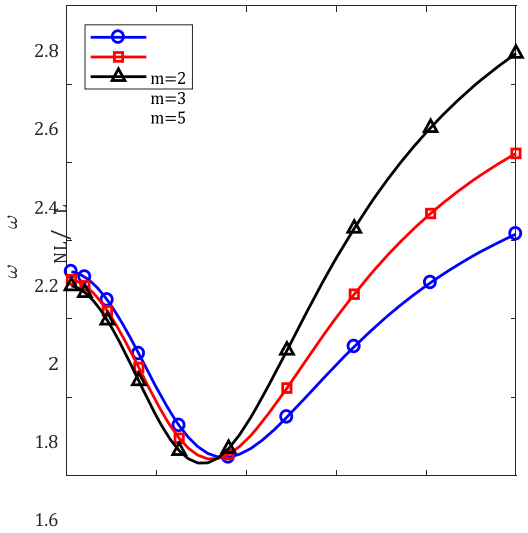

Figure 7 Aspect ratio effect on the nonlinear frequency ratio for different values of m (n=0)

In summary, the results of this research demonstrated that:

1. By increasing vibrations amplitude the nonlinear frequency increases, as well as the discrepancy between nonlinear and linear frequency is deeply depend on the vibration amplitude.
2. By increasing the gradient indexes results the reduction of nonlinear frequency.
3. Degree of hardening nonlinearity behavior of the 2D-FG plate is highly depend on the length and width FG indexes.
4. Aspect ratio have significant effects on the nonlinear frequency.
5. Modified Lindstedt-Poincare method is a powerful and easy tool for solving the strongly nonlinear equation. The results from analytical and numerical methods are in excellent agreements.

References

[1] Zhang, D.G., and Zhou, Y.H., "A Theoretical Analysis of FGM Thin Plates Based on Physical Neutral Surface", Comp. Mater. Sci. Vol. 44, pp. 716–720, (2008).

[2] Abrate, S., "Functionally Graded Plates Behave Like Homogeneous Plates", Compos. Part B-Eng. Vol. 39, pp. 151–158, (2008).

[3] Nguyen, T.K., Sab, K., and Bonnet, G., "First-order Shear Deformation Plate or Functionally Graded Materials", Compos. Struct. Vol. 83, pp. 25–36, (2008).

[4] Timoshenko, S.P., "On the Transverse Vibrations of Bars of Uniform Cross-section", Philos. Mag. Vol. 43, pp. 125–131, (1922).

[5] Ferreira, A.J.M., Batra, R.C., Roque, C.M.C., Qian, L.F., and Jorge, R.M.N., "Natural Frequencies of Functionally Graded Plates by a Meshless Method", Compos. Struct. Vol. 75, pp. 593–600, (2006).

[6] Efraim, E., and Eisenberger, M., "Exact Vibration Analysis of Variable Thickness Thick Annular Isotropic and FGM Plates", J. Sound Vib. Vol. 299, pp. 720–738, (2007).

[7] Thai, H. T., and Choi, D. H., “A Simple First-order Shear Deformation Theory for the Bending and Free Vibration Analysis of Functionally Graded Plates”, Composite Structures, Vol. 101, pp. 332-340, (2013).

[8] Abrate, S., “Free Vibration, Buckling, and Static Deflections of Functionally Graded Plates”, Compos. Sci. Technol. Vol. 66, pp. 2383–2394, (2006).

[9] Rani, R., and Lal, R., “Free Vibrations of Composite Sandwich Plates by Chebyshev Collocation Technique”, Composites Part B: Engineering, Vol. 165, pp. 442–455, (2019).

[10] Hosseini-Hashemi S., Taher, H.R., Akhavan, H., and Omidi, M., “Free Vibration of Functionally Graded Rectangular Plates using First-order Shear Deformation Plate Theory”, Applied Mathematical Modelling, Vol. 34, pp. 1276–1291, (2010).

[11] Zhao, X., Lee, Y.Y., and Liew, K.M., “Free Vibration Analysis of Functionally Graded Plates using the Element-free kp-Ritz Method”, Journal of Sound and Vibration, Vol. 319, pp. 918–939, (2009).

[12] Yang, J., and Shen, H.S., “Vibration Characteristics and Transient Response of Shear-deformable Functionally Graded Plates in Thermal Environments”, Journal of Sound and Vibration, Vol. 255, pp. 579–602, (2002).

[13] Gupta, A., Talha, M., and Singh, B.N., “Vibration Characteristics of Functionally Graded Material Plate with Various Boundary Constraints using Higher Order Shear Deformation Theory”, Composites Part B: Engineering, Vol. 94, pp. 64–74, (2016).

[14] Arefi, M., Mohammad-Rezaei Bidgoli, E., and Zenkour, A.M., "Free Vibration Analysis of a Sandwich Nano-plate Including FG Core and Piezoelectric Face-sheets by Considering Neutral Surface", Mechanics of Advanced Materials and Structures, Vol. 26, No. 9, pp. 741-752, (2019).

[15] Arefi, M., and Rabczuk, T., "A Nonlocal Higher Order Shear Deformation Theory for Electro-elastic Analysis of a Piezoelectric Doubly Curved Nano Shell", Composites Part B: Engineering, Vol. 168, pp. 496-510, (2019).

[16] Arefi, M., Mohammad-Rezaei Bidgoli, E., Dimitri, R., Bacciocchi, M., and Tornabene, F., "Application of Sinusoidal Shear Deformation Theory and Physical Neutral Surface to Analysis of Functionally Graded Piezoelectric Plate", Composites Part B: Engineering, Vol. 151, pp. 35-50 (2018).

[17] Arefi, M., and Zenkour, A.M., "Size-dependent Electro-elastic Analysis of a Sandwich Microbeam Based on Higher-order Sinusoidal Shear Deformation Theory and Strain Gradient Theory", Journal of Intelligent Material Systems and Structures, Vol. 29, No. 7 pp. 1394-1406, (2018).

[18] Wang, Y.Q., and Zu, J.W., “Large-amplitude Vibration of Sigmoid Functionally Graded Thin Plates with Porosities”, Thin-Walled Structures, Vol. 119, pp. 911–924, (2017).

[19] Yazdi, A.A., “Homotopy Perturbation Method for Nonlinear Vibration Analysis of Functionally Graded Plate”, Journal of Vibration and Acoustics, Vol. 135, pp. 12–21, (2013).

[20] Woo, J., Meguid, S.A., and Ong, L.S., "Nonlinear Free Vibration Behavior of Functionally Graded Plates", Journal of Sound and Vibration, Vol. 289, pp. 595–611, (2006).

[21] Malekzadeh, P., and Monajjemzadeh, S.M., "Nonlinear Response of Functionally Graded Plates under Moving Load", Thin-Walled Structures, Vol. 96, pp. 120–129, (2015).

[22] Duc, N.D., and Cong, P.H., "Nonlinear Vibration of Thick FGM Plates on Elastic Foundation Subjected to Thermal and Mechanical Loads using the First-order Shear Deformation Plate Theory", Cogent Engineering, Vol. 2, pp. 1045222, (2015).

[23] Fung, C.P., and Chen, C.S., "Imperfection Sensitivity in the Nonlinear Vibration of Functionally Graded Plates", European Journal of Mechanics-A/Solids, Vol. 25, pp. 425–461, (2006).

[24] Fakhari, V., Ohadi, A., and Yousefian, P., "Nonlinear Free and Forced Vibration Behavior of Functionally Graded Plate with Piezoelectric Layers in Thermal Environment", Composite Structures, Vol. 93, pp. 2310–2321, (2011).

[25] Hao, Y.X., Zhang, W., and Yang, J., "Nonlinear Oscillation of a Cantilever FGM Rectangular Plate Based on Third-order Plate Theory and Asymptotic Perturbation Method", Composites Part B: Engineering, Vol. 42, pp. 402–415, (2011).

[26] Zhang, W., Hao, Y., Guo, X., and Chen, L., "Complicated Nonlinear Responses of a Simply Supported FGM Rectangular Plate under Combined Parametric and External Excitations", Meccanica, Vol. 47, pp. 985–1014, (2012).

[27] Dinh Duc, N., Tuan, N.D., Tran, P., and Quan, T.Q., "Nonlinear Dynamic Response and Vibration of Imperfect Shear Deformable Functionally Graded Plates Subjected to Blast and Thermal Loads", Mechanics of Advanced Materials and Structures, Vol. 24, pp. 318-347, (2017).

[28] Şimşek, M., "Bi-directional Functionally Graded Materials (BDFGMs) for Free and Forced Vibration of Timoshenko Beams with Various Boundary Conditions", Composite Structures, Vol. 133, pp. 968-978, (2015).

[29] Tang, Y., and Ding, Q., "Nonlinear Vibration Analysis of a Bi-directional Functionally Graded Beam under Hygro-thermal Loads", Composite Structures, Vol. 225, pp. 111076, (2019).

[30] Fariborz, J., and Batra, R. C., "Free Vibration of Bi-directional Functionally Graded Material Circular Beams using Shear Deformation Theory Employing Logarithmic Function of Radius", Composite Structures, Vol. 210, pp. 217-230, (2019).

[31] Rajasekaran, S., and Khaniki, H. B., "Bi-directional Functionally Graded Thin-Walled Non-prismatic Euler Beams of Generic Open/Closed Cross Section Part I: Theoretical Formulations", Thin-Walled Structures, Vol. 141, pp. 627-645, (2019).

[32] Tang, Y., Lv, X., and Yang, T., "Bi-directional Functionally Graded Beams: Asymmetric Modes and Nonlinear Free Vibration", Composites Part B: Engineering, Vol. 156, pp. 319-331, (2019).

[33] Rajasekaran, S., and Khaniki, H. B., "Size-dependent Forced Vibration of Non-uniform Bi-directional Functionally Graded Beams Embedded in Variable Elastic Environment Carrying a Moving Harmonic Mass", Applied Mathematical Modelling, Vol. 72, pp. 129-154, (2019).

[34] Chen, M., Jin, G., Ma, X., Zhang, Y., Ye, T., and Liu, Z., "Vibration Analysis for Sector Cylindrical Shells with Bi-directional Functionally Graded Materials and Elastically Restrained Edges", Composites Part B: Engineering, Vol. 153, pp. 346-363, (2018).

[35] Chen, M., Jin, G., Ma, X., Zhang, Y., Ye, T., and Liu, Z., "Vibration Analysis for Sector Cylindrical Shells with Bi-directional Functionally Graded Materials and Elastically Restrained Edges", Composites Part B: Engineering, Vol. 153, pp. 346-363, (2018).

[36] Lieu, Q. X., Lee, D., Kang, J., and Lee, J., "NURBS-based Modeling and Analysis for Free Vibration and Buckling Problems of In-plane Bi-directional Functionally Graded Plates", Mechanics of Advanced Materials and Structures, Vol. 26, No. 12, pp. 1064-1080, (2019).

[37] Lieu, Q. X., Lee, S., Kang, J., and Lee, J., "Bending and Free Vibration Analyses of In-plane Bi-directional Functionally Graded Plates with Variable Thickness using Isogeometric Analysis", Composite Structures, Vol. 192, pp. 434-451, (2018).

[38] Wu, C. P., and Yu, L. T., "Free Vibration Analysis of Bi-directional Functionally Graded Annular Plates using Finite Annular Prism Methods", Journal of Mechanical Science and Technology, Vol. 33, No. 5, pp. 2267-2279, (2019).

[39] Kumar, Y., and Lal, R., "Prediction of Frequencies of Free Axisymmetric Vibration of Two-directional Functionally Graded Annular Plates on Winkler Foundation", European Journal of Mechanics-A/Solids, Vol. 42, pp. 219-228, (2013).

[40] Shariyat, M., and Alipour, M. M., " Differential Transform Vibration and Modal Stress Analyses of Circular Plates Made of Two-directional Functionally Graded Materials Resting on Elastic Foundations", Archive of Applied Mechanics, Vol. 81, No. 9, pp. 1289-1306, (2011).

[41] Alipour, M. M., Shariyat, M., and Shaban, M., "A Semi-analytical Solution for Free Vibration of Variable Thickness Two-directional-functionally Graded Plates on Elastic Foundations", International Journal of Mechanics and Materials in Design, Vol. 6, No. 4, pp. 293-304, (2010).

[42] Aragh, B. S., Hedayati, H., Farahani, E. B., and Hedayati, M., "A Novel 2-D Six-parameter Power-law Distribution for Free Vibration and Vibrational Displacements of Two-dimensional Functionally Graded Fiber-reinforced Curved Panels", European Journal of Mechanics-A/Solids, Vol. 30, No. 6, pp. 865-883, (2011).

[43] Kumar, Y., "Free Vibration of Two-directional Functionally Graded Annular Plates using Chebyshev Collocation Technique and Differential Quadrature Method", International Journal of Structural Stability and Dynamics, Vol. 15, No. 06, pp. 1450086, (2015).

[44] Lal, R., and Ahlawat, N., "Buckling and Vibrations of Two-directional Functionally Graded Circular Plates Subjected to Hydrostatic In-plane Force", Journal of Vibration and Control, Vol. 23, No. 13, pp. 2111-2127, (2017).

[45] Lal, R., and Ahlawat, N., "Buckling and Vibrations of Two-directional FGM Mindlin Circular Plates under Hydrostatic Peripheral Loading", Mechanics of Advanced Materials and Structures, Vol. 26, No. 3, pp. 199-214, (2019).

[46] Shariyat, M., and Alipour, M. M., "A Power Series Solution for Vibration and Complex Modal Stress Analyses of Variable Thickness Viscoelastic Two-directional FGM Circular Plates on Elastic Foundations", Applied Mathematical Modelling, Vol. 37, No. 5, pp. 3063-3076, (2013).

[47] Tahouneh, V., and Naei, M. H., "A Novel 2-D Six-parameter Power-law Distribution for Three-dimensional Dynamic Analysis of Thick Multi-directional Functionally Graded Rectangular Plates Resting on a Two-parameter Elastic Foundation", Meccanica, Vol. 49, No. 1, pp. 91-109, (2014).

[48] Tahouneh, V., and Yas, M. H., "Semianalytical Solution for Three-dimensional Vibration Analysis of Thick Multidirectional Functionally Graded Annular Sector Plates under Various Boundary Conditions", Journal of Engineering Mechanics, Vol. 140, No. 1, pp. 31-46, (2013).

[49] Yas, M. H., and Moloudi, N., "Three-dimensional Free Vibration Analysis of Multi-directional Functionally Graded Piezoelectric Annular Plates on Elastic Foundations Via State Space Based Differential Quadrature Method", Applied Mathematics and Mechanics, Vol. 36, No. 4, pp. 439-464, (2015).

[50] Reddy, J. N., "*Theory and Analysis of Elastic Plates and Shells*", CRC Press, New York, (2006).

[51] Chia, C.Y., "*Nonlinear Analysis of Plates*", McGraw-Hill International Book Company, New York, (1980).

[52] Reddy, J.N., "*Mechanics of Laminated Composite Plates and Shells: Theory and Analysis*", CRC Press, New York, (2004).

[53] Nayfeh, A.H., and Mook, D.T., "*Nonlinear Oscillation*", John Wiley & Sons, Inc, New York, (1995).

[54] He, J.H., "Modified Lindstedt–Poincare Methods for Some Strongly Non-linear Oscillations: Part I: Expansion of a Constant", International Journal of Non-Linear Mechanics, Vol. 37, pp. 309-314, (2002).

Nomenclature

A Non-dimensional maximum vibration amplitude
E_c Modulus of elasticity of ceramic
E_m Modulus of elasticity of metal

I Mass inertia related term
M Moment resultant
N Force resultant
P Material properties
Q Stiffness coefficient
p Half wave number (y-direction)
q Half wave number (x-direction)
$\emptyset_x$ Rotation about the y axes
$\emptyset_y$ Rotation about the x axes
U Virtual strain energy
V Virtual work done by applied forces
K Virtual kinetic energy
u_0 Displacements of any point on the middle surface of the plate in the x direction
v_0 Displacements of any point on the middle surface of the plate in the y direction
w_0 Displacements of any point on the middle surface of the plate in the z direction

Greek Symbols

ρ_c Density of ceramic
ρ_m Density of metal
ε Normal strain
γ Shear strain
τ Shear stress
σ Normal stress
ν Poisson's ratio
ϵ Book keeping parameter
ω_L Linear natural frequency
ω_{NL} Nonlinear natural frequency

Appendix. A

$$C_{11} = -\frac{1}{8r^3(\nu^2-1)}\pi^2 \int_0^1 \int_0^1 \cos(\pi\bar{x})\sin(\pi\bar{y})(2\pi\sin(2\pi\bar{x})(s^2\nu + (s^2+1)\cos(2\pi\bar{y}) - 1)\bar{E}(\bar{x},\bar{y}) + s^2(-(\nu-1))\sin(2\pi\bar{x})\sin(2\pi\bar{y})\frac{\partial\bar{E}(\bar{x},\bar{y})}{\partial\bar{y}} + 4(s^2\nu\sin^2(\pi\bar{x})\cos^2(\pi\bar{y}) + \cos^2(\pi\bar{x})\sin^2(\pi\bar{y}))\frac{\partial\bar{E}(\bar{x},\bar{y})}{\partial\bar{x}})\, d\bar{y}\, d\bar{x}$$

$$C_{12} = \frac{1}{2r^2(\nu^2-1)}\pi \int_0^1 \int_0^1 \cos(\pi\bar{x})\sin(\pi\bar{y})(s^2(\nu-1)\cos(\pi\bar{x})\cos(\pi\bar{y})\frac{\partial\bar{E}(\bar{x},\bar{y})}{\partial\bar{y}} - \pi(s^2(\nu-1) - 2)\cos(\pi\bar{x})\sin(\pi\bar{y})\bar{E}(\bar{x},\bar{y}) + 2\sin(\pi\bar{x})\sin(\pi\bar{y})\frac{\partial\bar{E}(\bar{x},\bar{y})}{\partial\bar{x}})\, d\bar{y}\, d\bar{x}$$

$$C_{13}=\int_0^1\int_0^1(-\frac{\pi^2 s\nu\cos^2(\pi\bar{x})\sin^2(\pi\bar{y})\bar{E}(\bar{x},\bar{y})}{r^2(1-\nu^2)}-\frac{\pi s\nu\sin(\pi\bar{x})\cos(\pi\bar{x})\sin^2(\pi\bar{y})\frac{\partial\bar{E}(\bar{x},\bar{y})}{\partial\bar{x}}}{r^2(1-\nu^2)}$$
$$-\frac{\pi^2 s\cos^2(\pi\bar{x})\sin^2(\pi\bar{y})\bar{E}(\bar{x},\bar{y})}{2r^2(\nu+1)}+\frac{\pi s\cos^2(\pi\bar{x})\sin(\pi\bar{y})\cos(\pi\bar{y})\frac{\partial\bar{E}(\bar{x},\bar{y})}{\partial\bar{y}}}{2r^2(\nu+1)})\,d\bar{y}\,d\bar{x}$$

$$C_{21}=\frac{1}{8r^3(\nu^2-1)}\pi^2 s\int_0^1\int_0^1\sin(\pi\bar{x})\cos(\pi\bar{y})(-2\pi\sin(2\pi\bar{y})((s^2+1)\cos(2\pi\bar{x})-s^2+\nu)\bar{E}(\bar{x},\bar{y})$$
$$-4(s^2\sin^2(\pi\bar{x})\cos^2(\pi\bar{y})+\nu\cos^2(\pi\bar{x})\sin^2(\pi\bar{y}))\frac{\partial\bar{E}(\bar{x},\bar{y})}{\partial\bar{y}}+(\nu$$
$$-1)\sin(2\pi\bar{x})\sin(2\pi\bar{y})\frac{\partial\bar{E}(\bar{x},\bar{y})}{\partial\bar{x}})\,d\bar{y}\,d\bar{x}$$

$$C_{22}=\int_0^1\int_0^1(-\frac{\pi^2 s\nu\sin^2(\pi\bar{x})\cos^2(\pi\bar{y})\bar{E}(\bar{x},\bar{y})}{r^2(1-\nu^2)}-\frac{\pi s\nu\sin^2(\pi\bar{x})\sin(\pi\bar{y})\cos(\pi\bar{y})\frac{\partial\bar{E}(\bar{x},\bar{y})}{\partial\bar{y}}}{r^2(1-\nu^2)}$$
$$-\frac{\pi^2 s\sin^2(\pi\bar{x})\cos^2(\pi\bar{y})\bar{E}(\bar{x},\bar{y})}{2r^2(\nu+1)}+\frac{\pi s\sin(\pi\bar{x})\cos(\pi\bar{x})\cos^2(\pi\bar{y})\frac{\partial\bar{E}(\bar{x},\bar{y})}{\partial\bar{x}}}{2r^2(\nu+1)})\,d\bar{y}\,d\bar{x}$$

$$C_{23}=\int_0^1\int_0^1(-\frac{\pi^2 s^2\sin^2(\pi\bar{x})\cos^2(\pi\bar{y})\bar{E}(\bar{x},\bar{y})}{r^2(1-\nu^2)}-\frac{\pi s^2\sin^2(\pi\bar{x})\sin(\pi\bar{y})\cos(\pi\bar{y})\frac{\partial\bar{E}(\bar{x},\bar{y})}{\partial\bar{y}}}{r^2(1-\nu^2)}$$
$$-\frac{\pi^2\sin^2(\pi\bar{x})\cos^2(\pi\bar{y})\bar{E}(\bar{x},\bar{y})}{2r^2(\nu+1)}+\frac{\pi\sin(\pi\bar{x})\cos(\pi\bar{x})\cos^2(\pi\bar{y})\frac{\partial\bar{E}(\bar{x},\bar{y})}{\partial\bar{x}}}{2r^2(\nu+1)})\,d\bar{y}\,d\bar{x}$$

$$C_{31}=\int_0^1\int_0^1\sin^2(\pi\bar{x})\sin^2(\pi\bar{y})\bar{\rho}(\bar{x},\bar{y})\,d\bar{y}\,d\bar{x}$$

$$C_{32}=\int_0^1\int_0^1(\frac{\pi^2 s^2\sin^2(\pi\bar{x})\sin^2(\pi\bar{y})\bar{E}(\bar{x},\bar{y})}{2r^2(\nu+1)}-\frac{\pi s^2\sin^2(\pi\bar{x})\sin(\pi\bar{y})\cos(\pi\bar{y})\frac{\partial\bar{E}(\bar{x},\bar{y})}{\partial\bar{y}}}{2r^2(\nu+1)}$$
$$+\frac{\pi^2\sin^2(\pi\bar{x})\sin^2(\pi\bar{y})\bar{E}(\bar{x},\bar{y})}{2r^2(\nu+1)}-\frac{\pi\sin(\pi\bar{x})\cos(\pi\bar{x})\sin^2(\pi\bar{y})\frac{\partial\bar{E}(\bar{x},\bar{y})}{\partial\bar{x}}}{2r^2(\nu+1)})\,d\bar{y}\,d\bar{x}$$

$$C_{33}=\frac{1}{8r^3(\nu^2-1)}\pi^2\int_0^1\int_0^1\sin(\pi\bar{x})\sin(\pi\bar{y})(-2\pi((s^2(\nu-1)+2)\cos(2\pi\bar{x})+3s^2\nu\cos(2\pi\bar{y})$$
$$-s^2\cos(2\pi(\bar{x}+\bar{y}))-(s^2+1)\cos(2\pi(\bar{x}-\bar{y}))-s^2\cos(2\pi\bar{y})-\cos(2\pi(\bar{x}+\bar{y})))\bar{E}(\bar{x},\bar{y})$$
$$+s^2\sin(2\pi\bar{y})((\nu+1)\cos(2\pi\bar{x})-3\nu+1)\frac{\partial\bar{E}(\bar{x},\bar{y})}{\partial\bar{y}}-\sin(2\pi\bar{x})((s^2(\nu-1)$$
$$-2)\cos(2\pi\bar{y})+s^2(\nu-1)+2)\frac{\partial\bar{E}(\bar{x},\bar{y})}{\partial\bar{x}})\,d\bar{y}\,d\bar{x}$$

$$C_{34}=\frac{1}{8r^3(\nu^2-1)}\pi^2 s\int_0^1\int_0^1 \sin(\pi\bar{x})\sin(\pi\bar{y})(2\pi(s^2\cos(2\pi(\bar{x}+\bar{y}))+(s^2+1)\cos(2\pi(\bar{x}-\bar{y}))$$
$$-2s^2\cos(2\pi\bar{y})+(1-3\nu)\cos(2\pi\bar{x})-\nu\cos(2\pi\bar{y})+\cos(2\pi(\bar{x}+\bar{y}))$$
$$+\cos(2\pi\bar{y}))\bar{E}(\bar{x},\bar{y})+\sin(2\pi\bar{y})((2s^2-\nu+1)\cos(2\pi\bar{x})-2s^2-\nu+1)\frac{\partial\bar{E}(\bar{x},\bar{y})}{\partial\bar{y}}$$
$$+\sin(2\pi\bar{x})((\nu+1)\cos(2\pi\bar{y})-3\nu+1)\frac{\partial\bar{E}(\bar{x},\bar{y})}{\partial\bar{x}})\,d\bar{y}\,d\bar{x}$$

$$C_{35}=\int_0^1\int_0^1(\frac{3\pi^4s^4\sin^4(\pi\bar{x})\sin^2(\pi\bar{y})\cos^2(\pi\bar{y})\bar{E}(\bar{x},\bar{y})}{2r^4(1-\nu^2)}-\frac{\pi^3s^4\sin^4(\pi\bar{x})\sin(\pi\bar{y})\cos^3(\pi\bar{y})\frac{\partial\bar{E}(\bar{x},\bar{y})}{\partial\bar{y}}}{2r^4(1-\nu^2)}$$
$$-\frac{2\pi^4s^2\nu\sin^2(\pi\bar{x})\cos^2(\pi\bar{x})\sin^2(\pi\bar{y})\cos^2(\pi\bar{y})\bar{E}(\bar{x},\bar{y})}{r^4(1-\nu^2)}$$
$$+\frac{\pi^4s^2\nu\sin^4(\pi\bar{x})\sin^2(\pi\bar{y})\cos^2(\pi\bar{y})\bar{E}(\bar{x},\bar{y})}{2r^4(1-\nu^2)}+\frac{\pi^4s^2\nu\sin^2(\pi\bar{x})\cos^2(\pi\bar{x})\sin^4(\pi\bar{y})\bar{E}(\bar{x},\bar{y})}{2r^4(1-\nu^2)}$$
$$-\frac{\pi^3s^2\nu\sin^3(\pi\bar{x})\cos(\pi\bar{x})\sin^2(\pi\bar{y})\cos^2(\pi\bar{y})\frac{\partial\bar{E}(\bar{x},\bar{y})}{\partial\bar{x}}}{2r^4(1-\nu^2)}$$
$$-\frac{\pi^3s^2\nu\sin^2(\pi\bar{x})\cos^2(\pi\bar{x})\sin^3(\pi\bar{y})\cos(\pi\bar{y})\frac{\partial\bar{E}(\bar{x},\bar{y})}{\partial\bar{y}}}{2r^4(1-\nu^2)}$$
$$-\frac{2\pi^4s^2\sin^2(\pi\bar{x})\cos^2(\pi\bar{x})\sin^2(\pi\bar{y})\cos^2(\pi\bar{y})\bar{E}(\bar{x},\bar{y})}{r^4(\nu+1)}$$
$$+\frac{\pi^4s^2\sin^4(\pi\bar{x})\sin^2(\pi\bar{y})\cos^2(\pi\bar{y})\bar{E}(\bar{x},\bar{y})}{2r^4(\nu+1)}+\frac{\pi^4s^2\sin^2(\pi\bar{x})\cos^2(\pi\bar{x})\sin^4(\pi\bar{y})\bar{E}(\bar{x},\bar{y})}{2r^4(\nu+1)}$$
$$-\frac{\pi^3s^2\sin^3(\pi\bar{x})\cos(\pi\bar{x})\sin^2(\pi\bar{y})\cos^2(\pi\bar{y})\frac{\partial\bar{E}(\bar{x},\bar{y})}{\partial\bar{x}}}{2r^4(\nu+1)}$$
$$-\frac{\pi^3s^2\sin^2(\pi\bar{x})\cos^2(\pi\bar{x})\sin^3(\pi\bar{y})\cos(\pi\bar{y})\frac{\partial\bar{E}(\bar{x},\bar{y})}{\partial\bar{y}}}{2r^4(\nu+1)}$$
$$+\frac{3\pi^4\sin^2(\pi\bar{x})\cos^2(\pi\bar{x})\sin^4(\pi\bar{y})\bar{E}(\bar{x},\bar{y})}{2r^4(1-\nu^2)}-\frac{\pi^3\sin(\pi\bar{x})\cos^3(\pi\bar{x})\sin^4(\pi\bar{y})\frac{\partial\bar{E}(\bar{x},\bar{y})}{\partial\bar{x}}}{2r^4(1-\nu^2)})\,d\bar{y}\,d\bar{x}$$

$$C_{36}=\int_0^1\int_0^1(\frac{\pi\sin^2(\pi\bar{x})\sin^2(\pi\bar{y})\bar{E}(\bar{x},\bar{y})}{2r(\nu+1)}-\frac{\sin(\pi\bar{x})\cos(\pi\bar{x})\sin^2(\pi\bar{y})\frac{\partial\bar{E}(\bar{x},\bar{y})}{\partial\bar{x}}}{2r(\nu+1)})\,d\bar{y}\,d\bar{x}$$

$$C_{37}=\int_0^1\int_0^1(\frac{\pi s\sin^2(\pi\bar{x})\sin^2(\pi\bar{y})\bar{E}(\bar{x},\bar{y})}{2r(\nu+1)}-\frac{s\sin^2(\pi\bar{x})\sin(\pi\bar{y})\cos(\pi\bar{y})\frac{\partial\bar{E}(\bar{x},\bar{y})}{\partial\bar{y}}}{2r(\nu+1)})\,d\bar{y}\,d\bar{x}$$

$$C_{41}=\frac{\pi\int_0^1\int_0^1\cos^2(\pi\bar{x})\sin^2(\pi\bar{y})\bar{E}(\bar{x},\bar{y})\,d\bar{y}\,d\bar{x}}{2r\nu+2r}$$

$$C_{42}=\frac{1}{24r^2(\nu^2-1)}(\int_0^1\int_0^1\cos(\pi\bar{x})\sin(\pi\bar{y})(\cos(\pi\bar{x})\sin(\pi\bar{y})(12r^2(\nu-1)+\pi^2(s^2(\nu-1)-2))\bar{E}(\bar{x},\bar{y})$$
$$+\pi(s^2(-(\nu-1))\cos(\pi\bar{x})\cos(\pi\bar{y})\frac{\partial\bar{E}(\bar{x},\bar{y})}{\partial\bar{y}}-2\sin(\pi\bar{x})\sin(\pi\bar{y})\frac{\partial\bar{E}(\bar{x},\bar{y})}{\partial\bar{x}}))\,d\bar{y}\,d\bar{x})$$

$$C_{43}=\int_0^1\int_0^1\Big(\frac{\pi^2 s\nu\cos^2(\pi\bar{x})\sin^2(\pi\bar{y})\bar{E}(\bar{x},\bar{y})}{12r^2(1-\nu^2)}+\frac{\pi s\nu\sin(\pi\bar{x})\cos(\pi\bar{x})\sin^2(\pi\bar{y})\frac{\partial\bar{E}(\bar{x},\bar{y})}{\partial\bar{x}}}{12r^2(1-\nu^2)}$$
$$+\frac{\pi^2 s\cos^2(\pi\bar{x})\sin^2(\pi\bar{y})\bar{E}(\bar{x},\bar{y})}{24r^2(\nu+1)}-\frac{\pi s\cos^2(\pi\bar{x})\sin(\pi\bar{y})\cos(\pi\bar{y})\frac{\partial\bar{E}(\bar{x},\bar{y})}{\partial\bar{y}}}{24r^2(\nu+1)}\Big)\,d\bar{y}\,d\bar{x}$$

$$C_{51}=\frac{\pi s\int_0^1\int_0^1\sin^2(\pi\bar{x})\cos^2(\pi\bar{y})\bar{E}(\bar{x},\bar{y})\,d\bar{y}\,d\bar{x}}{2r\nu+2r}$$

$$C_{52}=\int_0^1\int_0^1\Big(\frac{\pi^2 s\nu\sin^2(\pi\bar{x})\cos^2(\pi\bar{y})\bar{E}(\bar{x},\bar{y})}{12r^2(1-\nu^2)}+\frac{\pi s\nu\sin^2(\pi\bar{x})\sin(\pi\bar{y})\cos(\pi\bar{y})\frac{\partial\bar{E}(\bar{x},\bar{y})}{\partial\bar{y}}}{12r^2(1-\nu^2)}$$
$$+\frac{\pi^2 s\sin^2(\pi\bar{x})\cos^2(\pi\bar{y})\bar{E}(\bar{x},\bar{y})}{24r^2(\nu+1)}-\frac{\pi s\sin(\pi\bar{x})\cos(\pi\bar{x})\cos^2(\pi\bar{y})\frac{\partial\bar{E}(\bar{x},\bar{y})}{\partial\bar{x}}}{24r^2(\nu+1)}\Big)\,d\bar{y}\,d\bar{x}$$

$$C_{53}=-\frac{1}{24r^2(\nu^2-1)}\Big(\int_0^1\int_0^1\sin(\pi\bar{x})\cos(\pi\bar{y})\big(\sin(\pi\bar{x})\cos(\pi\bar{y})(\pi^2(2s^2-\nu+1)-12r^2(\nu-1))\bar{E}(\bar{x},\bar{y})$$
$$+\pi\big(2s^2\sin(\pi\bar{x})\sin(\pi\bar{y})\frac{\partial\bar{E}(\bar{x},\bar{y})}{\partial\bar{y}}+(\nu-1)\cos(\pi\bar{x})\cos(\pi\bar{y})\frac{\partial\bar{E}(\bar{x},\bar{y})}{\partial\bar{x}}\big)\big)\,d\bar{y}\,d\bar{x}\Big)$$

Appendix. B

$$\alpha=\frac{(-C_{37}C_{42}C_{51}+C_{36}C_{43}C_{51}+C_{37}C_{41}C_{52}-C_{32}C_{43}C_{52}-C_{36}C_{41}C_{53}+C_{32}C_{42}C_{53})}{C_{31}(-C_{43}C_{52}+C_{42}C_{53})}$$

$$\gamma=\frac{(C_{13}C_{21}C_{33}+C_{11}C_{23}C_{33}+C_{12}C_{21}C_{34}-C_{11}C_{22}C_{34}+C_{13}C_{22}C_{35}-C_{12}C_{23}C_{35})}{(C_{13}C_{22}-C_{12}C_{23})C_{31}}$$